Oxid Met (2011) 76:169–191
DOI 10.1007/s11085-011-9245-7

ORIGINAL PAPER

Comparative High Temperature Analysis of HVOF-Sprayed and Detonation Gun Sprayed Ni–20Cr Coating in Laboratory and Actual Boiler Environments

G. Kaushal · H. Singh · S. Prakash

Received: 31 October 2010 / Revised: 4 March 2011 / Published online: 22 March 2011

Abstract High-velocity-oxy-fuel (HVOF) spray and detonation-gun (D-gun) spray techniques were used to deposit Ni–20Cr coatings on a commonly used boiler steel ASTM-SAE 213-T22. The specimens, with and without coating, were subjected to molten salt (Na_2SO_4–60%V_2O_5) deposition in a laboratory furnace at 900 °C to determine hot-corrosion resistance. Specimens were also exposed to the superheater zone of a thermal power plant boiler at an average temperature of 700 °C under cyclic conditions to ascertain their erosion-corrosion (E-C) behavior. Mass-change measurements were taken to approximate the kinetics of corrosion and erosion-corrosion. In the case of E-C, the thickness lost data were also taken at the end of the exposure. The exposed specimens were characterized by X-ray diffraction (XRD) and field-emission scanning electron microscopy/energy dispersive spectroscopy (FE-SEM/EDS). The HVOF-sprayed coating was found to be intact during exposure to both given environments; whereas the D-gun coating showed spallation of its oxide scale during exposure to the molten salt environments. An overall analysis of the results indicated that the HVOF-sprayed Ni–20Cr coating should be a better choice for the given boiler applications.

Keywords Over-lay coating · Erosion-corrosion · Hot-corrosion · Protective coating · Boiler environment

G. Kaushal (✉)
RIMT-Institute of Engineering & Technology Mandi Gobindgarh, Punjab, India
e-mail: gagankaushal@rimt.ac.in

H. Singh
Indian Institute of Technology Ropar, Rupnagar, Punjab, India

S. Prakash
Indian Institute of Technology Roorkee, Roorkee, Uttarakhand, India

Introduction

The performance of materials used in high-temperature environments is related to their ability to form protective oxide scales on their surfaces. Considering economic aspects, the use of protective surface layers on high-temperature materials has attracted attention of many industries and has become a subject of many scientific investigations. In power-plant boilers, due to the threatened depletion of high grade fuels and for economic advantages, the use of residual fuels is well known. These residual fuels contain sodium, vanadium and sulphur as impurities, which when reacted with oxygen induce accelerated oxidation as their products melt at comparatively lower temperatures. Metals and alloys experience accelerated oxidation when their surfaces are covered with a thin film of a fused salt in an oxidizing environment at elevated temperatures. This mode of attack is commonly known as hot-corrosion, which takes place at an accelerated rate [1]. A common manifestation of hot-corrosion at elevated temperatures is the development of a porous non-protective oxide scale and sulphide precipitates in the substrate [2]. The most common deposit found on boiler super-heaters is the sodium vanadyl vanadate, $Na_2O{\cdot}V_2O_4{\cdot}5V_2O_5$, which melts at a relatively low temperature (550 °C). Above the melting point, this ash material corrodes metals by long-term contact [3]. One of the protective means to counteract the problem of high-temperature degradation is to coat the base material with a protective layer using various surface treatment techniques. A composite system of a base material providing the necessary mechanical strength with a protective surface layer different in structure and/or chemical composition and supplied by a surface treatment can be an optimum choice in combining materials properties [4].

Thermal spray techniques have been considered extensively to produce coatings for both performance and life enhancement of the engineering components [5–7]. There has been an increasing need to incorporate coatings as part of the component design and not as a 'repair' or 'afterthought' overlay [8].

In this work, two variants of thermal spraying, namely HVOF and D-gun have been used to develop protective coatings for the given boiler steel. Coatings produced by HVOF-spray have lower porosity, higher hardness, superior bond strength and less decarburization than many of the other thermal spraying methods [9–11]. Detonation-gun spraying (D-Gun) can achieve a temperature as high as 3850 °C in the combustion, and accelerate powder particles to a speed of 600 to 1200 m/s, which is much higher than that of low pressure Plasma Spraying (about 400 m/s) and High-Velocity Oxy-Fuel spraying (at maximum 500 m/s) [12]. As a result, the detonation spray coating gets a denser microstructure.

The aim of the current study is to investigate the comparative high-temperature behaviour of HVOF and D-gun-spray Ni–20Cr coating on a commonly used boiler steel SAE 213-T22 (T22) subjected to cyclic thermal exposure in laboratory and actual boiler environments. There are only a few earlier studies which present a comparative performance data for the mentioned spray processes under the given environments of study. The Ni–20Cr coating has been selected since its coefficient of thermal expansion (CTE) value is $17.3 \times 10^{-6}\ C^{-1}$, which does not vary significantly from that of base steel value ($14.2 \times 10^{-6}\ C^{-1}$). Therefore, it is

anticipated that the coating will not lose its adherence with the base steel during the thermal cyclic exposures. The outcome of the study can be useful to select an appropriate thermal spraying process for boiler applications.

Experimental Procedures

Development of Coatings

Substrate Material

SAE 213-T22 (T22) boiler steel with chemical composition C 0.15, Mn 0.3–0.6, P 0.03 max, S 0.03 max, Si 0.5, Cr 1.9–2.6, Mo 0.87–1.13 and Fe 94.66 (weight %) has been chosen as substrate material in the current study. Specimens each measuring 20 mm × 15 mm × 5 mm approximately were cut from the fresh steel and polished down to 180 grit SiC paper finish. They were subsequently grit blasted with Al_2O_3 (grit 60) before the deposition of the coatings by HVOF and D-gun-spraying.

Coating Formulation

Ni–20Cr powder was coated on the steel samples using a commercially available HVOF-spray (HIPOJET-2100) gun operating with oxygen and liquid petroleum gas (LPG) as input gases. The coating was deposited at Metallizing Equipment Company Private Limited, Jodhpur, India. The coating parameters adopted are reported in Table 1 [13]. Detonation-gun spray coatings were deposited at M/S Sai Surface Coating Technologies, Hyderabad, India. The coating parameters are mentioned in Table 2.

Characterization of as-sprayed Coatings

Details regarding the procedures adopted for the characterization of as-sprayed coatings have already been reported elsewhere [14].

Table 1 Spray parameters employed for HVOF coating [13]

Oxygen flow rate	200 SLPM
Fuel (LPG) flow rate	50 SLPM
Air-flow rate	900 SLPM
Spray distance	20 cm
Powder feed rate	25–30 g/min
Fuel pressure	6.00 kg/cm^2
Oxygen pressure	8.00 kg/cm^2
Air pressure	6.00 kg/cm^2

Table 2 Spray parameters employed for the D-gun coating

Parameter	Related value
Oxygen flow rate (kg/cm^2)	2640
C_2H_2 flow rate (kg/cm^2)	2240
N_2 flow rate (kg/cm^2)	960
Spray distance (mm)	140
Frequency of shots (s)	3

Molten Salt Corrosion Tests

Cyclic corrosion studies were performed in a molten salt environment consisting of a Na_2SO_4–60%V_2O_5 mixture (similar to the boiler environment salt deposit) for 50 cycles. Each cycle consisted of 1 h of heating at 900 °C in a silicon carbide tube furnace followed by 20 min of cooling at room temperature. A cyclic study of 50 cycles was performed as the duration of 50 h is considered to be adequate for attaining a steady state oxidation for a material [15]. The temperature of study was deliberately kept high (900 °C) as this will also take into consideration the overheating effects in case of boilers, which has been identified as the major cause of failure [16]. Moreover, at 900 °C, the rate of high-temperature hot-corrosion (HTHC) has been reported to be the severest [17]. It is anticipated that this thermal cyclic study shall also provide useful information regarding the adhesion and scale spallation tendency of the coating as per the suggestions of Burman and Ericsson [18].

The corrosion studies were performed on the uncoated as well as coated specimens for the purpose of comparison. Prior to the corrosion testing, the specimens were polished with SiC papers down to 1200 grit, which was followed by cloth wheel polishing with 1 μm alumina powder. This was done to obtain a consistent surface preparation for all the specimens. Salt mixture of Na_2SO_4–60%V_2O_5 was applied on the preheated specimens (250 °C) with a camel hairbrush. Attempts were made to achieve a uniform thickness of salt weighing 3 to 5 mg/cm^2. The mass-change measurements were taken at the end of each cycle with the help of an electronic balance machine CB-120 (Contech, Mumbai, India) having a sensitivity of 10^{-3} g. The spalled scale was also included at the time of measuring mass-change to determine the total rate of corrosion. After the exposure, surface, as well as, cross-sectional analysis of the corroded samples was done by X-ray diffraction (XRD) and field-emission scanning electron microscopy/energy dispersive spectroscopy (FE-SEM/EDS). For the cross-sectional analysis, the corroded samples were sectioned and mounted in epoxy followed by mirror-finish polishing.

E-C Studies in Actual Environment

The details regarding the procedures adopted for E-C studies in actual environment have already been reported elsewhere [14]. The chemical analysis of the ash inside the said boiler has been reproduced in Table 2 [13] and that of flue gas in Table 3 [13]. The studies were done at Guru Gobind Singh Super Thermal Power Plant, Ropar, Punjab, India. The specimens were subjected to low temperature primary

Table 3 Chemical analysis of ash present in the boiler environment [13]

Constituent	Mass % age
Silica	54.7
Fe_2O_3	5.18
Al_2O_3–Fe_2O_3/Al_2O_3	29.56
CaO	1.48
MgO	1.45
SO_3	0.23
Na_2O	0.34
K_2O	1.35
Ignition loss	4.31

Table 4 Chemical analysis of flue gas present in the boiler environment [13]

Constituent	Value related
Volumetric flow	231 m^3/s
SO_X	236 mg/m^3
NO_X	1004 $\mu m/m^3$
CO_2	14–16.5%
O_2	2.5–5%
40% excess air was supplied to boiler for combustion of coal	

superheater zone in the boiler unit III with the help of stainless steel wire through the soot blower dummy points at 41 m height from the base of the boiler. The temperature of the hanging zone was about 700 ± 10 °C with full load of 210 MW. The samples were exposed for 15 cycles, each cycle consisting of 100 h exposure in the boiler followed by 1 h cooling in ambient air Table 4.

Results

Porosity and XRD Analysis of as-sprayed Coatings

Average value of apparent surface porosity of HVOF, as well as, and D-gun-spray Ni–20Cr coatings was found to be 1.6%. The XRD diffractogram of the HVOF-spray Ni–20Cr coating is shown in Fig. 1a, whereas, that of the detonation gun spray coating in Fig. 1b. The analysis indicates the formation of Ni as primary phase alongwith Cr as a secondary phase for both the cases. The results indicate the formation of γ-Ni phase in the coating compositions.

FE-SEM/EDS analysis of as-sprayed coatings

Surface Analysis

SEM micrograph showing the surface morphology of HVOF-spray Ni–20Cr coated T22 steel is shown in Fig. 2a. The microstructure consists of irregular size splats

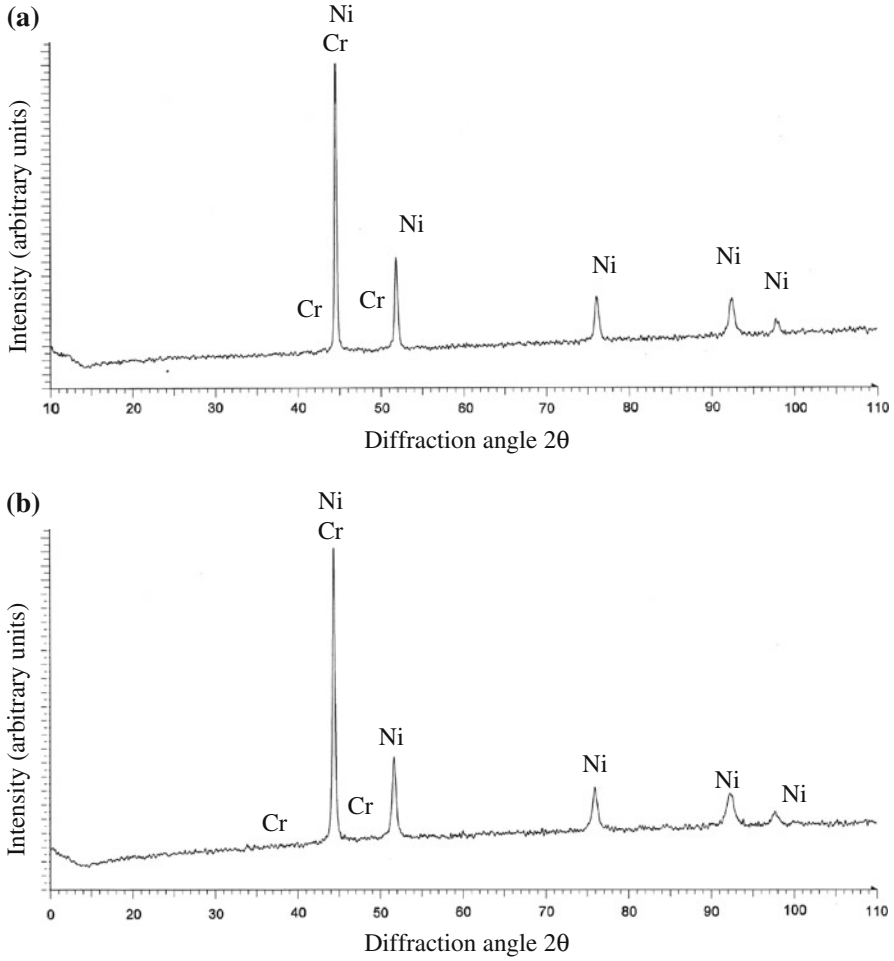

Fig. 1 XRD diffractogram for **a** HVOF-sprayed Ni–20Cr coating and **b** D-gun sprayed Ni–20Cr coating on T22 boiler steel

with flattened appearance, which is a typical characteristic of thermal spray coatings. There is a presence of some superficial microvoids in the microstructure. EDS measurements taken at the points 1 and 2 on the surface of the coating indicate a nearly uniform composition with Ni and Cr as main elements. This composition is nearly similar to that of the feedstock powder. A corresponding SEM micrograph of the D-gun- spray Ni–20Cr coated T22 steel is shown in Fig. 2b. The microstructure of the coating consists of irregular size splats. Comparatively larger splats are seen in the case of D-gun coating in comparison with the HVOF-sprayed coating.

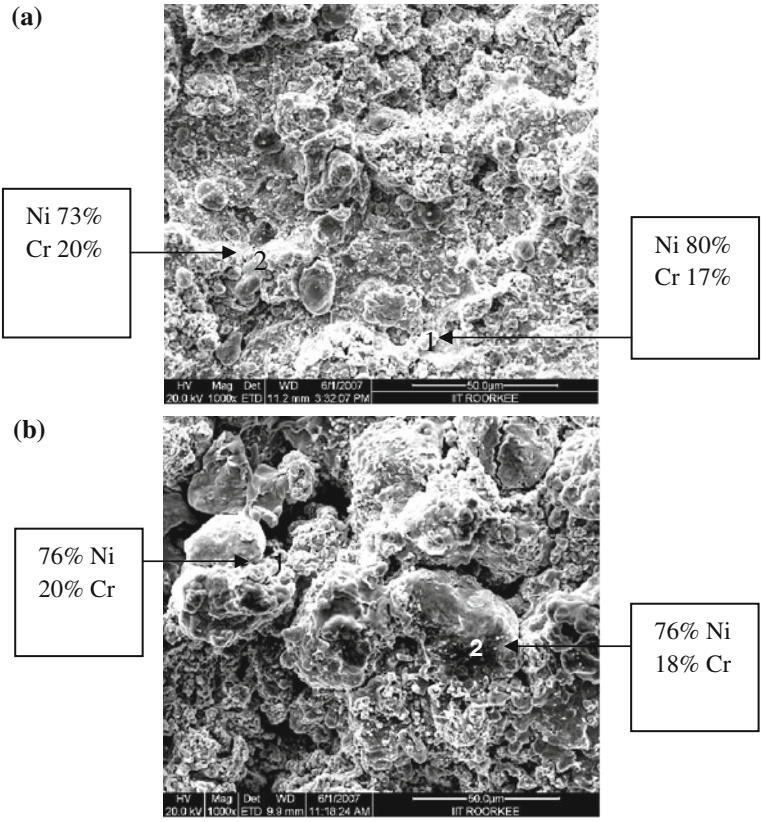

Fig. 2 Surface morphology and FE-SEM/EDS analysis for the **a** HVOF-sprayed Ni–20Cr coating and **b** D-gun sprayed Ni–20Cr coating on T22 boiler steel

Molten Salt Corrosion Tests and E-C Studies

Kinetics

Mass-change data in mg/cm^2 as a function of number of cycles for the uncoated, HVOF and D-gun-spray coated T22 steel subjected to Na_2SO_4–60%V_2O_5 environment at 900 °C for 50 cycles have been compiled in Fig. 3a. This mass-change data serve as a good index to compare the corrosion rates under similar conditions of exposure. It is obvious from the figure that the uncoated steel has shown much higher corrosion rates in comparison with its coated counterparts. The uncoated steel has shown the tendency to conceive mass gain continuously without showing any indication of steady state corrosion rate, whereas after the deposition of the coatings, the mass gains have reduced significantly. Moreover, the HVOF-sprayed steel showed a comparatively better corrosion resistance in comparison with D-gun-sprayed steel.

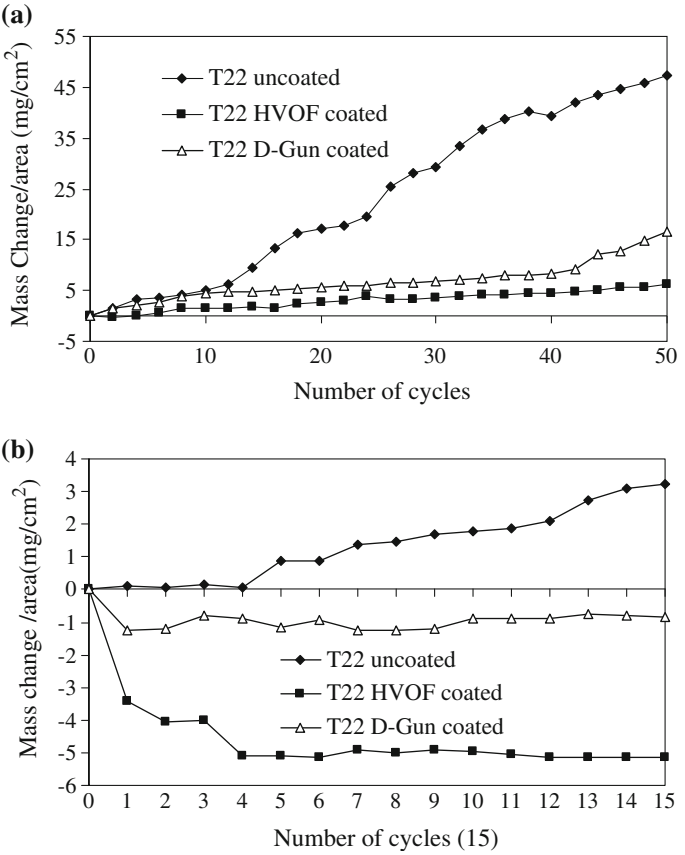

Fig. 3 Mass change versus number of cycle's plots for the uncoated, HVOF-sprayed Ni–20Cr coated and D-gun sprayed Ni–20Cr coated T22 steel subjected to **a** Na_2SO_4–60%V_2O_5 environment at 900 °C for 50 cycles and **b** E-C for 15 cycles in actual boiler environment at 700 °C

Comparative analyses indicate that the HVOF-sprayed steel seems to have achieved a steady state of reaction, whereas the D-gun-sprayed steel has shown somewhat higher reaction rates after 42nd cycle. It is worthwhile to mention that spallation of oxide scale was also observed after the end of 42nd cycle. The scale started to fall in the form of tiny flakes in the boat during the remaining cycles of the exposure. However, no such spallation or even crack formation was seen in the case of HVOF-sprayed steel. This indicates towards the effectiveness of the coating to prevent the oxidation of substrate steel, as the cyclic oxidation behaviour of an alloy is dictated mainly by scale spallation resistance as per the opinion of Stott [19]. Talking quantitatively, the mass gains for the steel got reduced by 87 and 65% after the application of HVOF and D-gun-spray coatings respectively.

During the exposure to actual boiler environment, the mass-changes, Fig. 3b, for the bare steel are only marginal for first four cycles of erosion-corrosion (E-C); thereafter noticeable mass-gains have been observed for the entire period of study.

These mass- gains may be due to two reasons; (1) the process might have taken place by the growth of oxide scales, and/or (2) accumulation of fly ash particles on the surfaces of the steel specimen. On the other hand, mass-losses have been observed for the coated steel samples. Furthermore, these losses have been observed during the initial cycles of exposure only. In the case of D-gun-sprayed sample, only a marginal loss has been recorded after the first cycle, thereafter the mass losses have become negligible. In the case of HVOF-sprayed sample, comparatively higher mass-losses have been observed till the end of fourth cycle, beyond which no mass-changes have been observed. These conditions of negligible mass-changes indicate towards steady state of E-C phenomena, which predicts that the coatings can be useful to protect the steel during longer durations of usage.

The extent of erosion-corrosion has also been measured in terms of thickness gained/lost after 1500 h of the exposure. The thickness gain for the uncoated substrate was 0.24 mm (55 mpy). In the case of HVOF-sprayed coating, thickness loss was 0.10 mm and in the D-gun coated substrate thickness loss of 0.065 mm was recorded. The corresponding erosion-corrosion rate expressed in mils per year (mpy) is found to be 23 mpy for HVOF-sprayed steel and 15 mpy for the D-gun coated steel.

XRD Analysis of the Exposed Specimens

The XRD patterns of the uncoated, HVOF-sprayed and D-gun-sprayed Ni–20Cr coated T22 steel subjected to corrosion testing in the boiler environment (Na_2SO_4–60%V_2O_5) at 900 °C for 50 cycles have been depicted in Fig. 4a–c respectively. Oxide scale of the uncoated steel mainly comprises Fe_2O_3 phase. Some weak peaks corresponding to FeV_2O_4 and Cr_2O_3 are also observed. In the oxide scale of HVOF-sprayed Ni–20Cr coated T22 steel (Fig. 4b), NiO has been observed as a strong phase alongwith Fe_2O_3 phase. $NiCr_2O_4$, FeV_2O_4 and Cr_2O_3 are observed as medium intensity phases. On the other hand, the analysis for D-gun-sprayed steel (Fig. 4c) revealed the formation of NiO and Fe_2O_3 as strong phases, alongwith Cr_2O_3 and FeV_2O_4 as medium intensity phases and $NiCr_2O_4$ as a weak intensity phase.

During the exposure in the actual boiler environment for 15 cycles, the XRD patterns of the uncoated, HVOF-sprayed and D-gun-sprayed Ni–20Cr coated T22 steel have been depicted in Fig. 5a–c respectively. Oxide scale of the uncoated steel mainly comprise Fe_2O_3 phase alongwith Al_2O_3 phase. In the oxide scale of HVOF-sprayed Ni–20Cr coated T22 steel (Fig. 5b), NiO has been observed as a strong phase alongwith Cr_2O_3 as a secondary phase. Some weak peaks of Fe_2O_3 alongwith Al_2O_3 are also observed. On the other hand, the D-gun-sprayed steel is found to have NiO as a main phase (Fig. 5c). Cr_2O_3 and Fe_2O_3 alongwith Al_2O_3 were observed as secondary phases.

FE-SEM/EDS Analysis of Exposed Samples

Surface Analysis The surface FE-SEM/EDS analysis of the uncoated, HVOF-sprayed and D-gun-sprayed Ni–20Cr coated T22 steel subjected to corrosion testing in the Na_2SO_4–60%V_2O_5 environment at 900 °C for 50 cycles has been depicted in

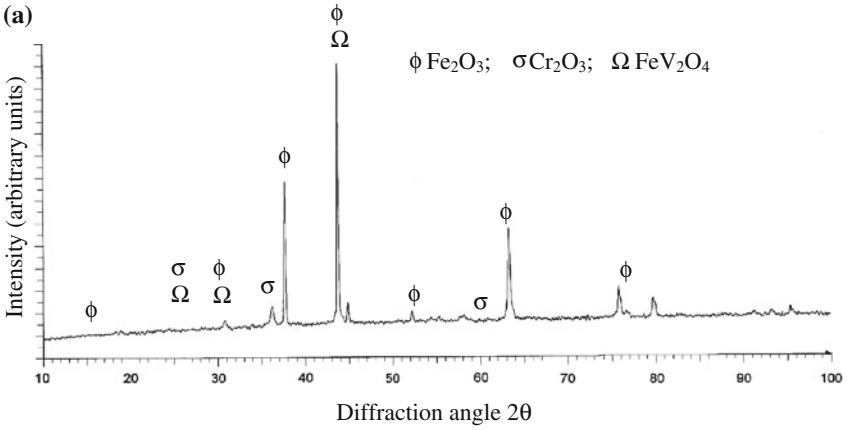
(a)
ϕ Fe2O3; σCr2O3; Ω FeV2O4
Intensity (arbitrary units)
Diffraction angle 2θ

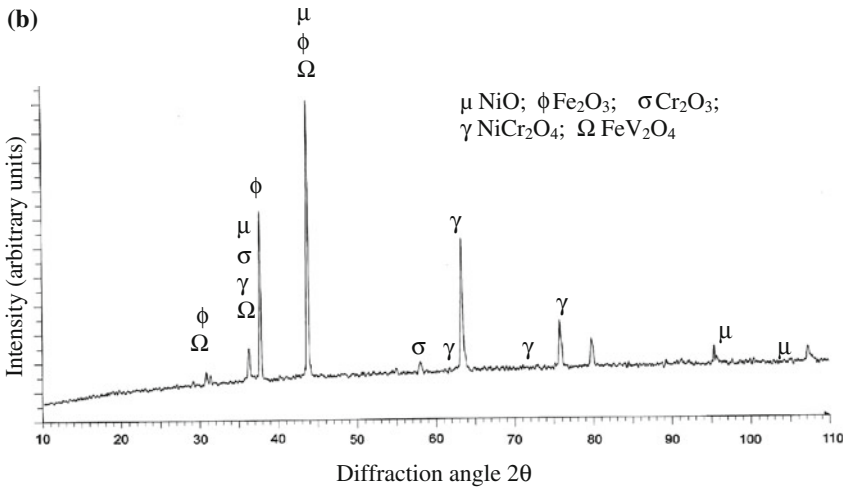
(b)
μ NiO; ϕ Fe2O3; σCr2O3;
γ NiCr2O4; Ω FeV2O4
Intensity (arbitrary units)
Diffraction angle 2θ

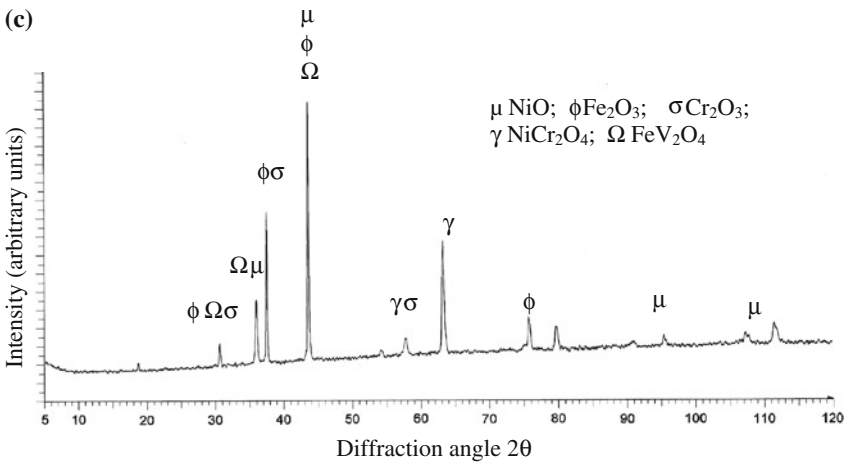
(c)
μ NiO; ϕFe2O3; σCr2O3;
γ NiCr2O4; Ω FeV2O4
Intensity (arbitrary units)
Diffraction angle 2θ

◀**Fig. 4** XRD diffractograms for the **a** uncoated, **b** HVOF-sprayed Ni–20Cr coated and **c** D-gun sprayed Ni–20Cr coated T22 steel subjected to Na_2SO_4–60%V_2O_5 environment at 900 °C for 50 cycles

Fig. 6a–c respectively. The oxide scale of the uncoated steel has a melted zone, which is mainly composed of Fe and O, thereby indicating the formation of Fe_2O_3-rich oxide scale. There is a significant presence of Mo in the scale composition. After the deposition of the HVOF-sprayed Ni–20Cr coating, the oxide scale has become crystalline (Fig. 6b). These crystals appear to be mainly of NiO as evidenced from the EDS analysis at points 1 and 2. The crystals of various sizes and shapes are visible distributed in the whole matrix. Similar results are obtained for the oxide scale of D-gun-sprayed Ni–20Cr coating (Fig. 6c).

During the exposure in the actual boiler environment for 15 cycles, the FE-SEM/EDS analysis of the uncoated, HVOF-sprayed and D-gun-sprayed Ni–20Cr coated T22 steel has been compiled in Fig. 7a–c respectively. The oxide scale for the bare T22 steel, Fig. 7a, has an upper sub-layer with a patchy appearance. The matrix mainly contains O, Fe, Si and Al alongwith C and V (ref point 1), whereas the point 2 on the upper sub-layer is mainly having O with lower amounts of Fe. Some amounts of Si, Al and C are also revealed alongwith minor amounts of V. It is pertinent to mention that the presence of elements such as Al, Si, and V in the oxide scales represents the accumulation of ash particles from the boiler environment. After the deposition of HVOF-sprayed Ni–20Cr coating, the upper sub-layer of the scale has a dense appearance, which is not continuous over the whole surface (Fig. 7b). This layer is consisting mainly of NiO. There is presence of some globular particles in the scale, which most probably are ash particles as could be perceived from presence of O, Si, Fe, S and Al elements in the scale composition. The oxide scale of D-gun-sprayed Ni–20Cr coating (Fig. 7c) has morphological features similar to the previous case. The scale comprises mainly Ni alongwith O at point 2, whereas at point 1 strong presence of Cr is observed. Si, Mg and Al are observed at the selected points representing the presence of ash particles that might have deposited from the boiler environment.

Cross-Sectional Analysis The SEI image showing the cross-sectional oxide scale morphology and corresponding EDS analysis at some selected points of the HVOF-coated and D-gun coated T22 steel subjected to Na_2SO_4–60%V_2O_5 environment at 900 °C for 50 cycles have been compiled in Fig. 8a, b respectively. The scale in this work has been referred to as the material present above the substrate steel, which may include oxidized/partially oxidized/unaffected coating layers plus any other layer found on the surface, as could be seen from the cross-sectional micrographs. In the case of HVOF-sprayed T22 steel, the coating seems to have retained its good adherence with the base metal even after the exposure (Fig. 8a). The amount of Ni after the interface point 2 has shown a decreasing trend as one move towards outer layers of the scale, whereas Cr has shown a mixed behaviour of high and low percentage along the thickness. Wherever Cr is richer, it is accompanied by the richness of O as well, thereby indicating the presence of Cr_2O_3. On the other hand; the amount of O is low at Ni-rich points. Fe is mainly restricted to the substrate steel, which indicates that the coating can act as barrier to the diffusion of the base

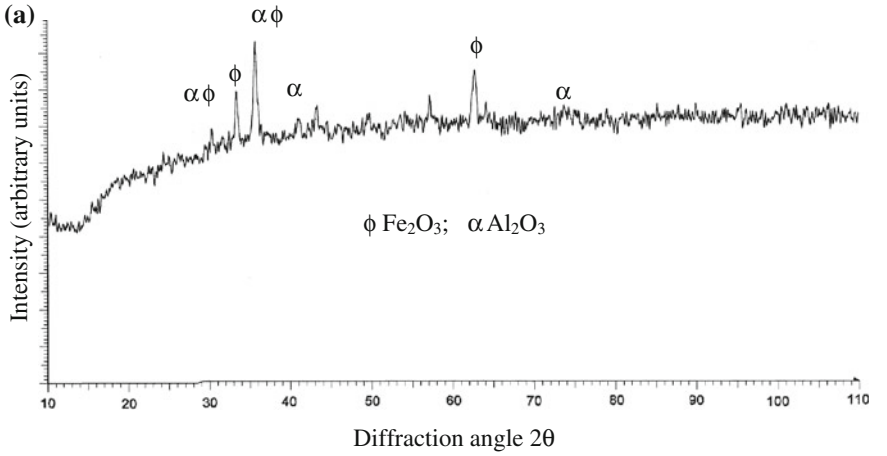
(a)
αϕ
ϕ
αϕ
α
ϕ
α
ϕ Fe2O3; α Al2O3
Intensity (arbitrary units)
10 20 30 40 50 60 70 80 90 100 110
Diffraction angle 2θ

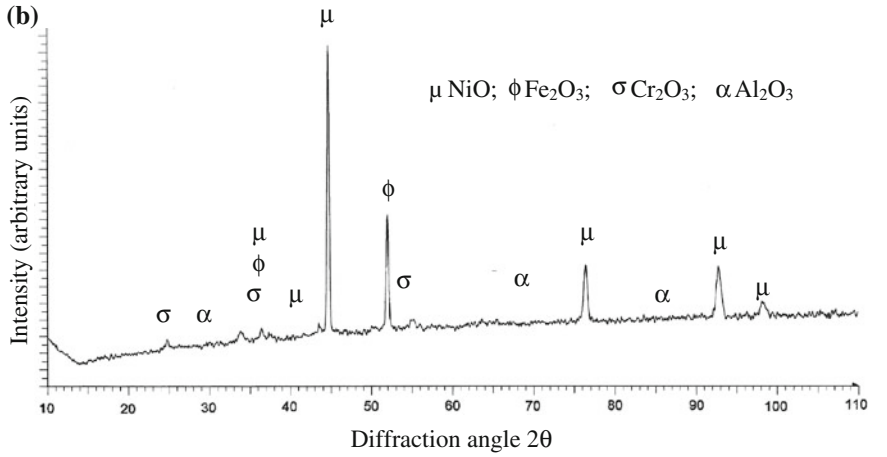
(b)
μ
μ NiO; ϕ Fe2O3; σ Cr2O3; α Al2O3
ϕ
μ
ϕ
σ
μ
σ
α
σ
α
μ
α
μ
α
μ
Intensity (arbitrary units)
10 20 30 40 50 60 70 80 90 100 110
Diffraction angle 2θ

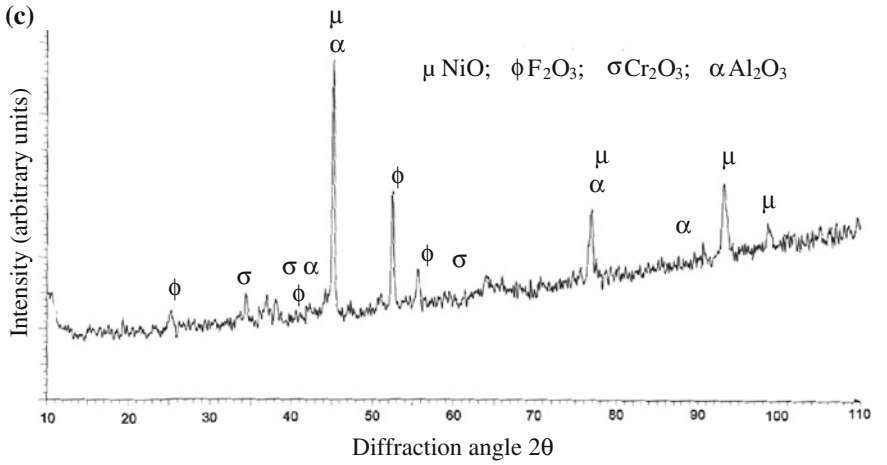
(c)
μ
α
μ NiO; ϕ F2O3; σ Cr2O3; α Al2O3
ϕ
μ
α
μ
α
μ
ϕ
ϕ
σ
σ α
ϕ
σ
Intensity (arbitrary units)
10 20 30 40 50 60 70 80 90 100 110
Diffraction angle 2θ

◀**Fig. 5** XRD diffractograms for the **a** uncoated **b** HVOF-sprayed Ni–20Cr coated and **c** D-gun sprayed Ni–20Cr coated T22 steel subjected to E-C for 15 cycles in actual boiler environment at 700° C

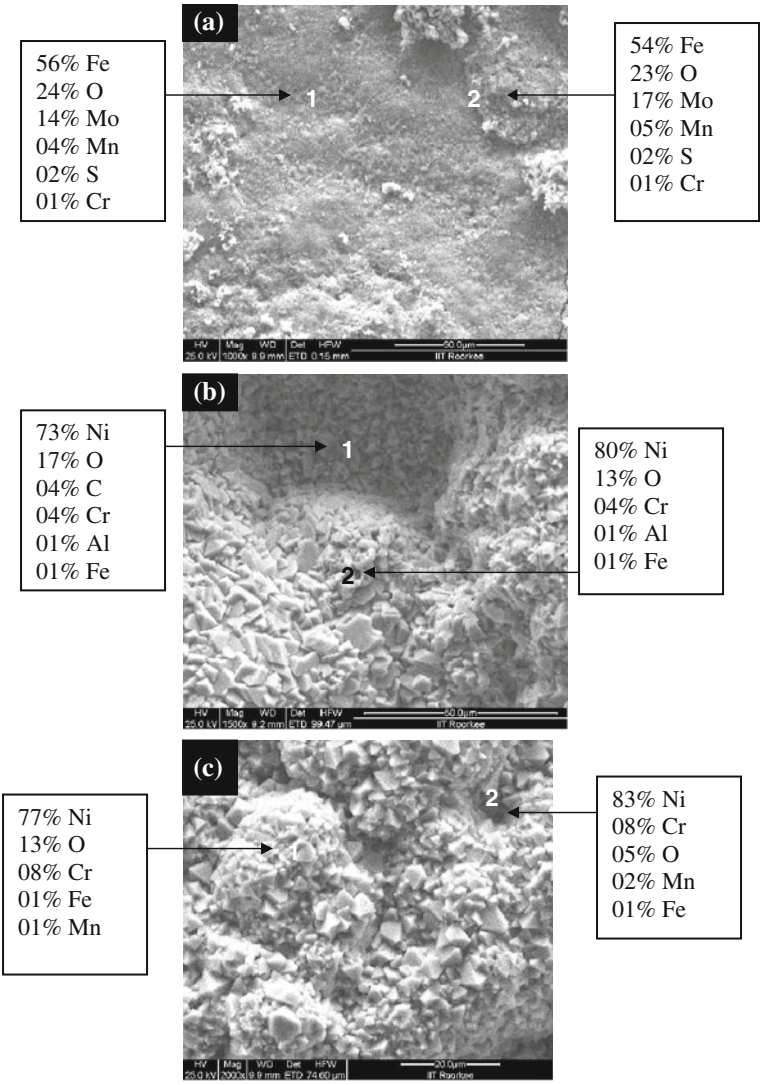

Fig. 6 Surface scale morphology and FE-SEM/EDS analysis for the **a** uncoated, **b** HVOF-sprayed Ni–20Cr coated and **c** D-gun sprayed Ni–20Cr coated T22 steel subjected to Na_2SO_4–60%V_2O_5 environment at 900 °C for 50 cycles

elements of the steel. In the case of D-gun coated steel (Fig. 8b), Ni and Cr have shown nearly uniform presence along the thickness of the scale. There is only marginal penetration of oxygen along the thickness of the scale, which indicates towards the effectiveness of the coating to act as a diffusion barrier to the corroding species.

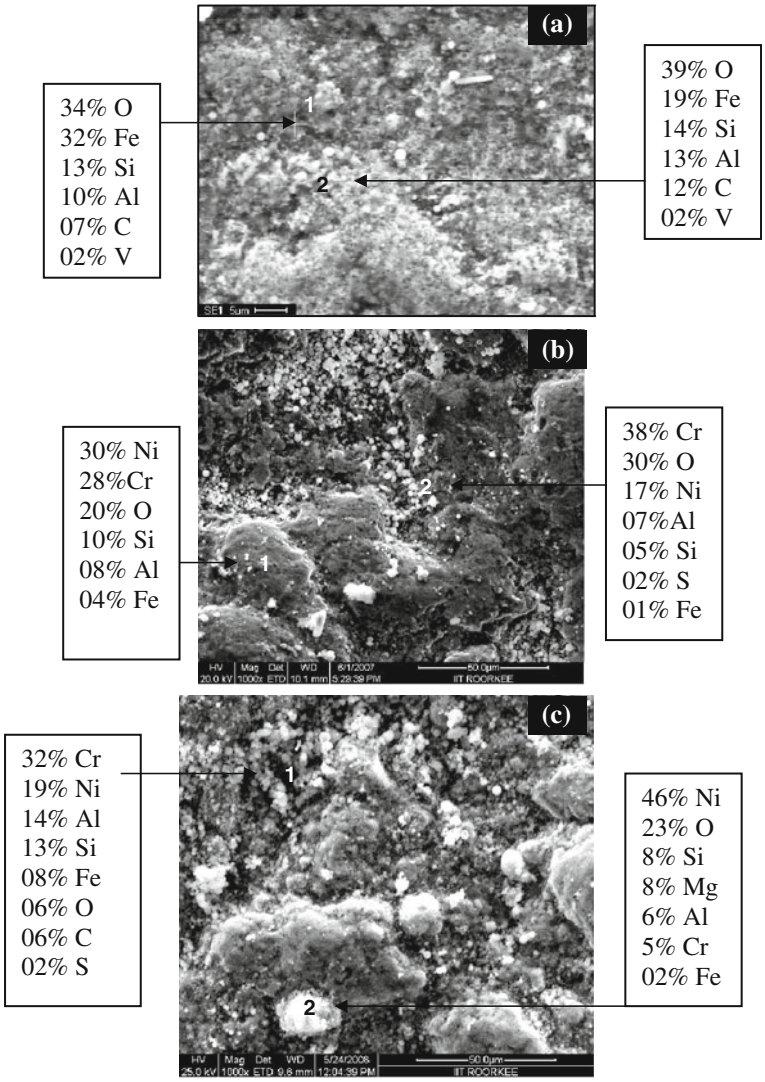

Fig. 7 Surface scale morphology and FE-SEM/EDS analysis for the **a** uncoated, **b** HVOF-sprayed Ni–20Cr coated and **c** D-gun sprayed Ni–20Cr coated T22 steel subjected to E-C for 15 cycles in actual boiler environment at 700 °C

In the case of HVOF-sprayed steel exposed to the actual boiler environment for 15 cycles, Fig. 9a, it is evident that the coating has retained its identity even after the exposure to the boiler environment for 1500 h. The scale is mainly rich in Ni and Cr. The penetration of oxygen along the coating cross-section is only marginal. Fe has diffused into the coating area up to point 2, beyond which Fe is almost absent. In the case of D-gun coated steel as shown in Fig. 9b, it has been observed that the coating has retained its identity. The composition of Ni has fallen from point

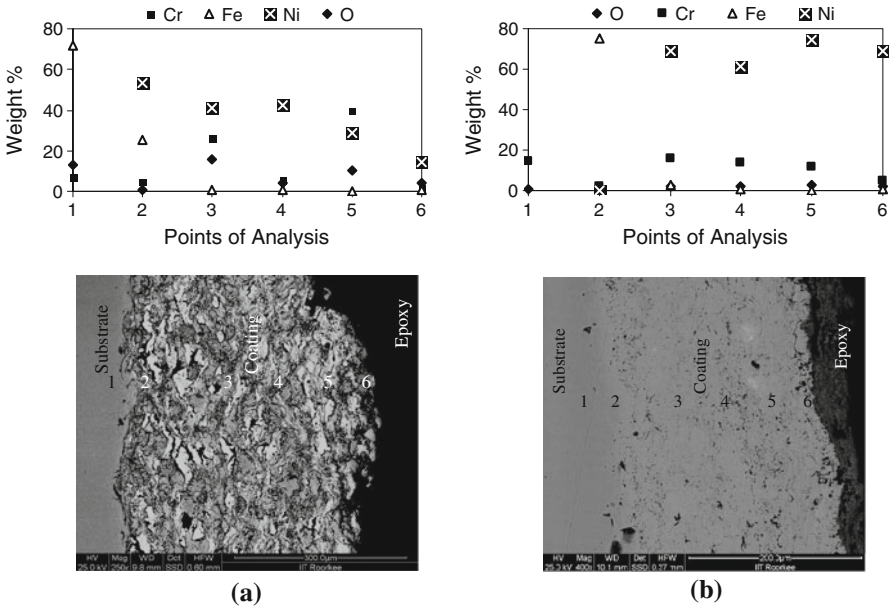

Fig. 8 Oxide scale morphology and elemental composition of the cross-section of the **a** HVOF-sprayed Ni–20Cr coated and **b** D-gun sprayed Ni–20Cr coated T22 steel subjected to Na_2SO_4–60%V_2O_5 environment at 900 °C for 50 cycles

2 onwards towards the outer layers of the scale, whereas the concentration of Cr has shown an increasing trend as one move towards the outer layers. It may be noted that the amount of O in the coating area in the case of D-gun-sprayed coated steel is more as compared to that in the case of HVOF-sprayed steel.

X-Ray Mappings of Exposed Specimens Composition image (SEI) and X-ray mappings of the cross-section of HVOF-spray and D-gun-spray coated T22 steel subjected to Na_2SO_4–60%V_2O_5 environment at 900 °C for 50 cycles have been compiled in Fig. 10a, b respectively. The analysis of the HVOF-sprayed steel (Fig. 10a) indicates that the base metal is mainly composed of Fe. The scale is composed mainly of Ni and Cr. There is the presence of some pure white regions in the scale, which are rich in Ni and are depleted of O and Cr. These are basically Ni-rich un-oxidized splats. The grey splats are containing both Ni as well as Cr. O, by and large, seems to be present along the splat boundaries. Fe is confined mainly to the substrate steel. Corresponding X-ray mappings of the exposed D-gun coated steel is shown in Fig. 10b. It is clearly revealed that the coating zone is mainly composed of Ni.

Composition image (SEI) and X-ray mappings of the cross-section of the HVOF coated and D-gun coated T22 steel subjected to the actual boiler environment after 15 cycles have been depicted in Fig. 11a, b respectively. In the case of HVOF-sprayed steel (Fig. 11a), it has been observed that Ni along with Cr dominates the scale composition which is consistent with the composition of the feedstock powder.

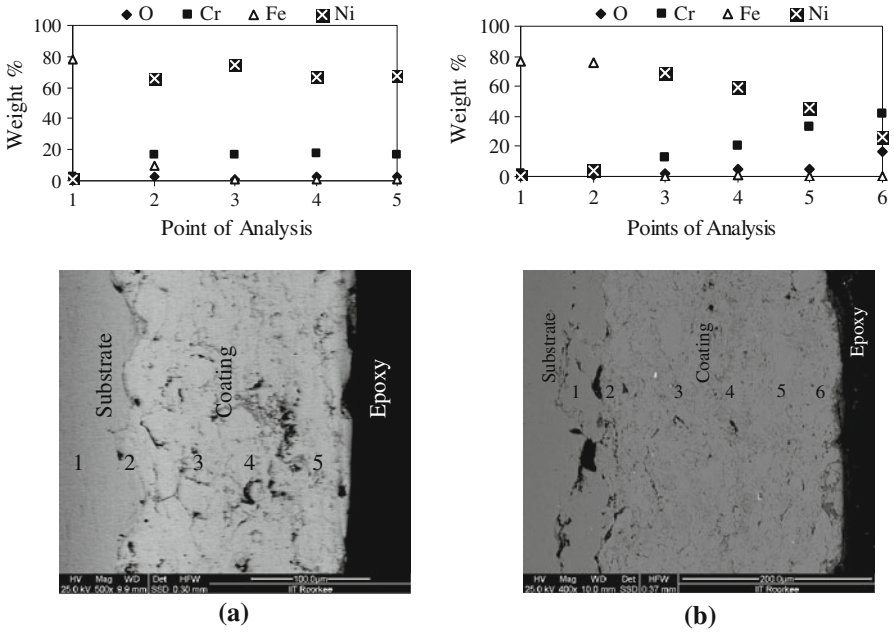

Fig. 9 Oxide scale morphology and elemental composition of the cross-section of the **a** HVOF-sprayed Ni–20Cr coated and **b** D-gun sprayed Ni–20Cr coated T22 steel subjected to actual boiler environment for 15 cycles

Oxygen attack seems very minimal as O is mainly present in the top layers of the oxide scales alongwith Cr, indicating the probable formation of protective oxide scales such as Cr_2O_3. There is the presence of a Cr-depleted band below this Cr_2O_3 layer. A Si-rich bed on the top of the scale reveals the presence of ash particles deposited during the exposure to the boiler. Almost similar results are observed in the case of D-gun-sprayed steel (Fig. 11b).

Discussion

Ni–20Cr powder was successfully deposited on the chosen T22 steel by the HVOF and D-gun-spray techniques using standard process parameters. The average thickness of the HVOF-sprayed coating was 160 μm and that of D-gun-sprayed coating was 125 μm. The measured values of porosity were similar in both types of coating. The measured porosity value was in good agreement with earlier studies on HVOF-spray coatings [20–23] and on D-gun-spray coatings by Rajasekaran et al. [24] and Kharlamov [25]. XRD analysis of the Ni–20Cr coating formed by both deposition techniques confirmed the presence of γ-Ni as the principal phase. The XRD results for both coating types are in good agreement with those reported earlier [26]. This was further confirmed by EDS analysis along surface (Fig. 2a, b), which showed the predominance of Ni in the coating together with Cr as a secondary element.

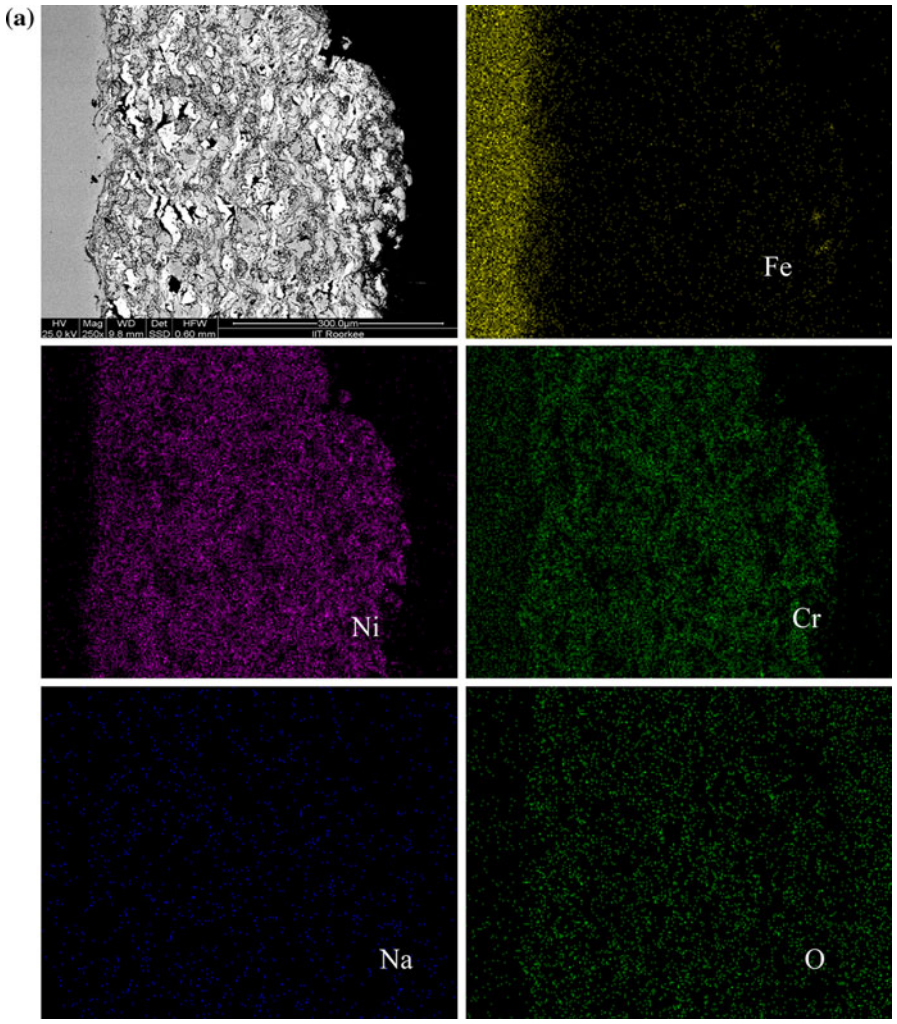

Fig. 10 Composition image (SEI) and X-ray mappings of the cross-section of **a** HVOF-sprayed Ni–20Cr coated and **b** D-gun sprayed Ni–20Cr coated T22 steel subjected to Na_2SO_4–60%V_2O_5 environment at 900 °C for 50 cycles

The uncoated steel, in general, showed higher rates of hot-corrosion in comparison with its coated counterparts (Fig. 3a). Kolta et al. [27] suggested that in the temperature range of 900 °C, the Na_2SO_4 and V_2O_5 will react to form $NaVO_3$ which acts as a catalyst and also serves as an oxygen carrier to the base alloy through the open pores present on the surface, which in turn leads to rapid oxidation of the base elements of the substrate. Fe_2O_3 was observed as a main phase in the oxide scale of the uncoated steel. This was further supported by FE-SEM/EDS analysis (Fig. 4a), which reveals higher amounts of Fe and O in the surface of scales of the uncoated substrate. The presence of Fe_2O_3 scale has been reported to be

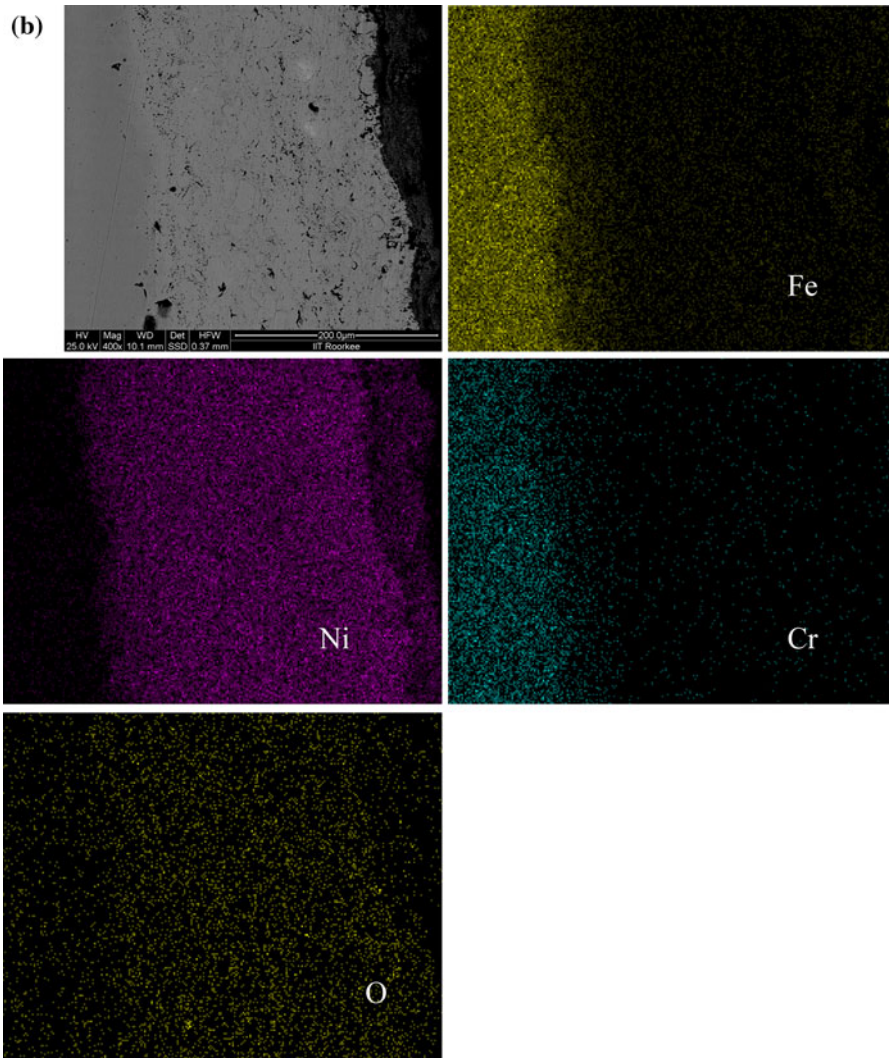

Fig. 10 continued

non-protective by Das et al. [28].The mass gains were substantially reduced after the applications of both the coatings. The HVOF-sprayed coating reduced the mass gain by 85% followed by D-gun coating which reduced the mass gain by 65%. In other words, the HVOF-spray technique looked to be a better choice in comparison with the D-gun technique from the standpoint of molten-salt corrosion resistance. The XRD analysis of both the coated T22 substrates (Fig. 4b and 4c) after corrosion studies revealed the presence of NiO phase alongwith Cr_2O_3 and $NiCr_2O_4$ phases. The latter oxides are known for providing superior corrosion resistance, as has been reported by others [29–31]. The surface FE-SEM/EDS analysis of the coated steel

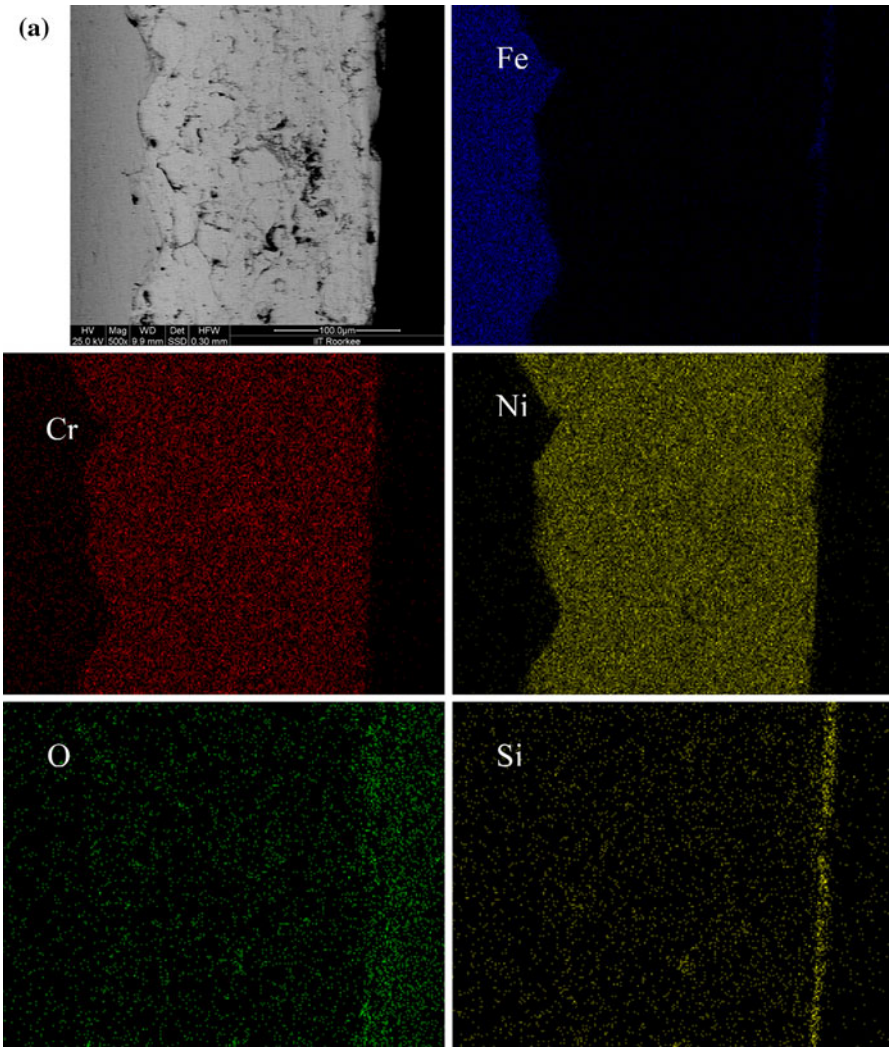

Fig. 11 Composition image (SEI) and X-ray mappings of the cross-section of the **a** HVOF-sprayed Ni–20Cr coated and **b** D-gun sprayed Ni–20Cr coated T22 steel subjected to subjected to actual boiler environment for 15 cycles

further supported the formation of these oxides (Fig. 6b, c).The results were confirmed by the cross-sectional analysis, which showed that the scale was mainly rich in Ni and Cr metal constituents. Moreover, the presence of a spinel phase in the oxide scale of the coated steel may further enhance the hot-corrosion resistance, as spinel phases have much lower diffusion coefficients of the cations and anions than those in the oxide phases of Fe [32].

During exposure in actual boiler environment the uncoated steel indicated mass gain (Fig. 3b); whereas, mass loss was observed after the application of both the

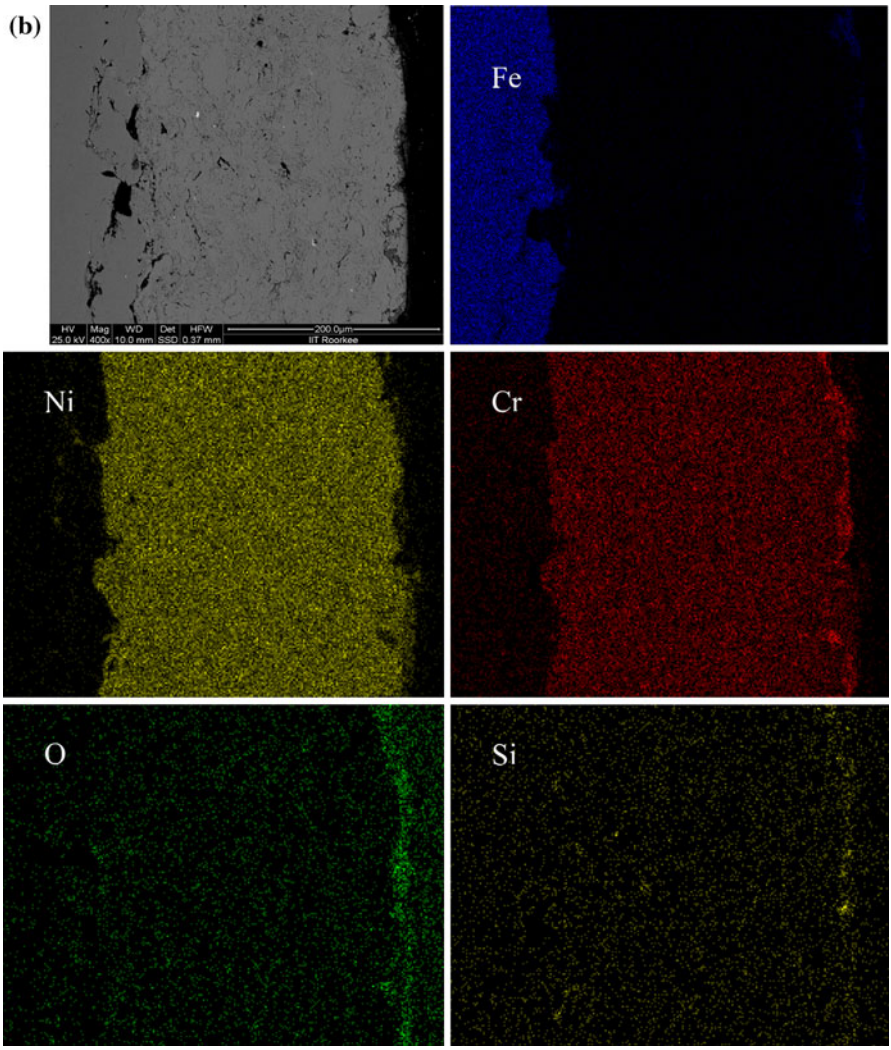

Fig. 11 continued

coatings. It has been observed that the E-C mass losses took place only during the initial four cycles (may be defined as transient period of E-C) of exposure in the boiler environment for both the coatings. This behaviour may be attributed to the erosion of micro-hills present on the coated samples. However, once the surfaces of the samples became smooth, no further erosion took place and the process achieved steady state conditions. The role of the coating is pronounced during the transient period of erosion during which it saved the substrate steel from the enhanced E-C loss. The mass loss recorded after the initial transient cycles for both the coatings was meager, which indicates that the coatings could be useful to reduce the

erosion-corrosion of the substrate steel during longer exposures in the actual boiler environment.

It has been reported that sigma (σ) phase is hard and fragile, in addition, when forms, it consumes chromium and molybdenum present within the matrix [33], which leads to the depletion in these elements and thereby prevent formation of Cr_2O_3. XRD analysis of the exposed coated specimens tested in the given environments indicated that no brittle (sigma) phase was formed in the scales. Cross-sectional analysis (Fig. 8, 9) and X-ray mappings (Figs. 10, 11), in general, revealed minor inter-diffusion of various elements between the substrate and the HVOF/D-gun-sprayed coatings. Minor inter-diffusion is reported to be beneficial [34] for providing better adhesion between the substrate and the coating. There was no spallation of the oxide scales, in general, during the exposure, except, in the case of D-gun-sprayed coating exposed to molten salt corrosion. In the latter case, spallation of oxide scale was observed during late hours of exposure. Since no spallation was observed in the HVOF-sprayed case, so mismatch in CTE cannot be the reason for this spallation, given that both the coating compositions are same.

The presence of NiO and Cr_2O_3 in the oxide scales of the coated steels in both the coatings (Fig. 5b, c) is indicative of providing a barrier to the base metal against any diffusion of oxidizing/corroding species. The presence of Al_2O_3 and SiO_2 phases in the oxide scales of both the uncoated and coated steels exposed to the boiler environment is attributable to the embedment of ash particles from the boiler environment.

Comparative results of both the coatings indicate that higher coating thickness was achieved by HVOF process, which is a desirable feature for E-C resistance. The results obtained after exposure in molten salt environment indicate that HVOF-sprayed coating reduced corrosion rates by higher amount than D-gun-spray coating. By contrast, during the E-C process, the D-gun coating showed lesser E-C rates during transient periods; however once the steady state conditions were reached, both the HVOF and D-gun-sprayed coatings showed negligible mass changes. In other words, the E-C performance of HVOF-sprayed coating is similar to that of D-gun-spray coating during longer duration of usage. Moreover, the HVOF-sprayed coating was found to be intact during exposure to both environments studied, whereas D-gun coating showed spallation of its oxide scale during the molten-salt deposition. Therefore, based on the overall analysis of the results obtained it can be anticipated that the HVOF-sprayed Ni–20Cr coating should be a better choice for the given boiler applications. Moreover, the HVOF-spray process provides the possibility of in-site applications for bigger installations.

Conclusions

1. The HVOF and D-gun-spraying techniques were used successfully to deposit Ni–20Cr on ASTM-SAE 213-T22 steel with the standard process parameters. The HVOF-spray process provided thicker coating in comparison with the D-gun-spray process.

2. The coatings were found to be useful to reduce the high-temperature corrosion rates of the steel in terms of mass-change and spallation tendency, when exposed to Na_2SO_4–60%V_2O_5 deposition at 900 °C. The HVOF-sprayed coating showed no spallation of its oxide scale, whereas the D-gun-sprayed coating exhibited spallation of its oxide scale.
3. Both the HVOF and D-gun-sprayed coatings were found to be useful to increase the E-C resistance of the steel in actual boiler environment. The coatings were found to retain their surface contact with the steels without any signs of scale spallation.
4. HVOF-sprayed Ni–20Cr coating is inferred be a better choice for the given boiler applications in comparison with the D-gun-sprayed Ni–20Cr coating in terms of better coating thickness and high-temperature behaviour.

References

1. N. Eliaz, G. Shemesh and R. M. Latanision, *Engineering Failure Analysis* **9**, 31 (2002).
2. R. A. Rapp, Y. S. Zhang, *JOM* **46**, 47 (1994).
3. M. M. Barbooti, S. H. Al-Madfai and J. Nassouri, *Thermochemica Acta* **126**, 43 (1988).
4. M. H. Li, X. F. Sun, J. G. Li, Z. Y. Zhang, T. Jin, H. R. Guan, and Z. Q. Hu, *Oxidation of Metals*, **59**, 591 (2003).
5. S. Watanabe and S. Yamamoto, *Materials Transactions Japan Institute of Metals* **47**, 26 (1977).
6. A. Motoki and M. Yoaiba, *Japan Society of Corrosion Engineering* **39**, 192 (1990).
7. Y. Matsubara, and A. Tomiguchi *Proceedings of 13th International Thermal Spray Conference* (Florida, USA, 1992), p. 637.
8. A. Vaidhya, T. Streibl, L. Li, S. Sampath, O. Kovarik and R. Greenlaw, *Materials Science and Engineering A* **403**, 191 (2005).
9. D. A. Stewart, P. H. Shipway and D. G. McCartney, *Wear* **225–229**, 789 (1999).
10. J. A. Picas, A. Forn, A. Igartua and G. Mendoza, *Surface and Coatings Technology* **174–175**, 1095 (2003).
11. S. Wirojanupatump, P. H. Shipway and D. G. McCartney, *Wear* **249**, 829 (2001).
12. Y. J. Zhang, X. F. Sun, Y. C. Zhang, T. Jin, C. G. Deng, H. R. Guan and Z. Q. Hu, *Materials Science and Engineering A* **360**, 65 (2003).
13. G. Kaushal, H. Singh, and S. Prakash, *Proceedings of International Thermal Spray Conference and Exposition* (The Netherlands, 2008), p. 1351.
14. G. Kaushal, H. Singh, and S. Prakash, *Metallurgical and Materials Transactions A* (Available online, 2011).
15. H. Singh, D. Puri and S. Prakash, *Surface and Coatings Technology* **192**, 27 (2005).
16. ASM International, *Metals Handbook*, Vol. 10 (ASM Publication, Metals Park OH, USA, 1975).
17. National Materials Advisory Board Report, *Coatings for High-Temperature Structural Materials: Trends and Opportunities*, (National Academy Press, Washington, DC, 1996).
18. C. Burman and T. Ericsson, *Proceedings of the Symposium High-Temperature Protective Coatings*, March 7–8, Atlanta, GA, USA, ed. S.C. Singhal (Metallurgical Society of AIME, Warrendale, PA, USA, 1983), p. 51.
19. F. H. Stott, *Materials Characterization* **28**, 311 (1992).
20. J. M. Miguel, J. M. Guilemany and S. Vizcaino, *Tribology International* **36**, 181 (2003).
21. T. Sahraoui, N. E. Fenineche, G. Montavon and C. Coddet, *Materials and Design* **24**, 309 (2003).
22. L. Gil and M. H. Staia, *Thin Solid Films* **420–421**, 446 (2002).
23. W. C. Lih, S. H. Yang, C. Y. Su, S. C. Huang, I. C. Hsu and M. S. Leu, *Surface and Coatings Technology* **133–134**, 54 (2000).
24. B. Rajasekaran, S. G. S. Raman, S. V. Joshi and S. Sundararajan, *Surface and Coatings Technology* **201**, 1548 (2006).

25. Y. A. Kharlamov, *Materials Science and Engineering* **93**, 1 (1987).
26. N. F. Ak, C. Tekmen, I. Ozdemir, H. S. Soykan and E. Celik, *Surface and Coatings Technology* **174–175**, 1070 (2003).
27. G. A. Kolta, I. F. Hewaidy and N. S. Felix, *Thermochimica Acta* **4**, 151 (1972).
28. D. Das, R. Balasubramaniam and M. N. Mungole, *Journal of Materials Science* **37**, 1135 (2002).
29. A. Ul-Hamid, *Materials Chemistry and Physics* **80**, 135 (2003).
30. T. S. Sidhu, R. D. Agrawal and S. Prakash, *Journal of Materials Engineering and Performance* **15**, 130 (2006).
31. T. Sundararajan, S. Kuroda, T. Itagaki and F. Abe, *ISIJ International* **43**, 104 (2003).
32. U. K. Chatterjee, S. K. Bose and S. K. Roy, *Environmental Degradation of Metals*, (Marcel Dekker, New York, 2001).
33. A. M. Babakr, et al., *Journal of Minerals & Materials Characterization & Engineering* **7**, 127 (2008).
34. J. R. Nicholls, *JOM* **52**, 28 (2000).